

Figure 2. CP2: charge pump with reduced undesired charge transfer [4].

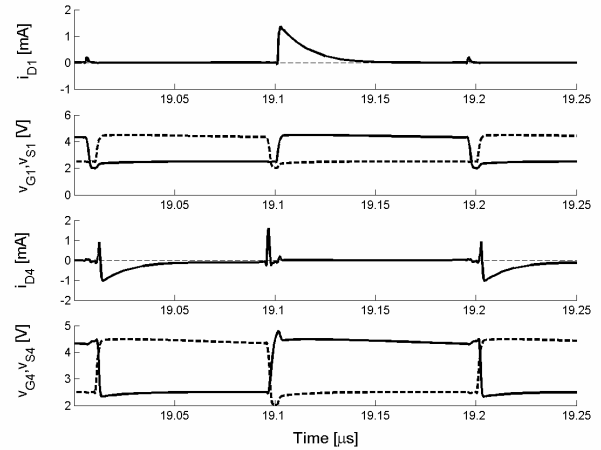


Figure 5. Simulated signals in the circuit in fig. 2.

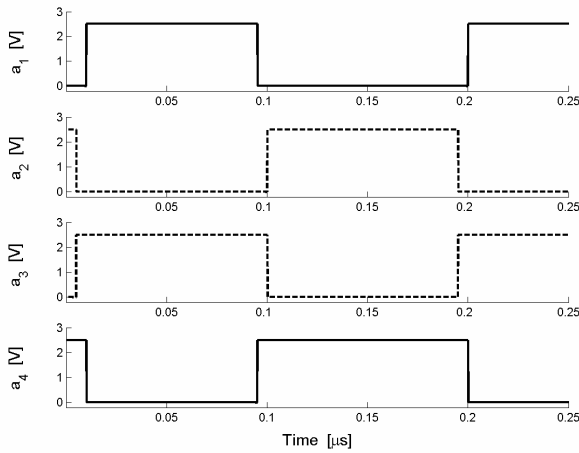


Figure 3. Control signals for the circuit in fig. 2.

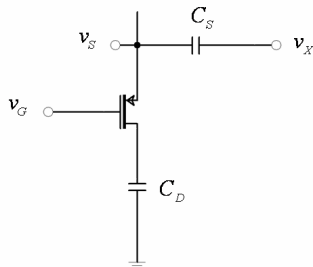


Figure 4. PMOS transistor in a charge pump.

A first solution has been proposed in [4] (see the circuit shown in fig. 2), where transistors M_9, M_{10}, M_{11} and M_{12} bias the n-well; control signals are shown in fig. 3. The undesired charge transfer is reduced, but not completely solved [4], as explained below.

Let us consider the PMOS transistor shown in fig. 4 (which is representative of PMOS transistors in the charge pump); the drain voltage is $2V_{DD}$. If the transistor is on and we want to switch it off, we must make sure that $v_G (L \rightarrow H)$ before the source voltage is changed (otherwise, if the transistor is still on even after the source voltage has already been changed, undesired charge transfer will occur). Similar considerations apply to the opposite transitions and for NMOS transistors. In summary:

- if a transistor (NMOS or PMOS) must be switched from on to off, its gate voltage must be (accordingly) changed *before* its source voltage is changed;
- if a transistor (NMOS or PMOS) must be switched from off to on, its gate voltage must be (accordingly) changed *after* its source voltage is changed.

These conditions are equivalent to the following one (much easier to be verified): the gate and the source voltages of NMOS transistors must be OV_L , whereas the gate and the source voltages of PMOS transistors must be OV_H . The previous analysis neglects the time for switching on and off the transistors and the parasitic capacitive paths to the bulk; however, generally, these effects give smaller contributions.

As to the circuit [4] (fig. 2), there is no undesired charge transfer in (M_1, M_2, M_7, M_8) , but there is undesired charge transfer in (M_3, M_4, M_5, M_6) ; this analysis is confirmed by simulations in fig. 5 (the current i_{D4} should always be *negative* as currents are considered positive when they enter the terminal).

III. CHARGE PUMP LESS SUSCEPTIBLE TO UNDESIRED CHARGE TRANSFER

Fig. 6 shows the proposed circuit; the transistors M_{33} and M_{44} are used for generating the signals (p_3, p_4) ; M_5 and M_6 bias the n-well. If the control signals depicted in fig. 7 are used, the conditions above discussed are satisfied for all transistors but M_{33} and M_{44} , which however may be very small (resulting in very little power losses). Fig. 8 confirms that the undesired charge transfer is greatly reduced.

In order to test the proposed solution, three fully integrated charge pumps have been designed in a standard $1.6\mu\text{m}$ CMOS process. In the first charge pump (fig. 1), the control signals (a_1, a_2) are OV_T (different conditions may easily lead to an even lower efficiency). In comparison with the classic voltage doubler, both the second circuit (fig. 2) and the third circuit (fig. 6) are expected to have a better light-load efficiency and an higher final output voltage (since undesired charge transfer also reduces the final output voltage). In all of the following simulations, a single parameter is changed while all the other parameters are set at their *reference value* (see table I). The three charge pumps have the same total area.

Fig. 9 shows the efficiency and the final output voltage as a function of the load resistance; the efficiency improvement is, clearly, more evident under light-load conditions.

Fig. 10 shows the efficiency and the final output voltage as a function of the width of the NMOS transistors (the width of the PMOS transistors has been changed according to $w_p = 2.3w_n$). Efficiency improvements are obtained only if the width of the transistors is sufficiently large (as this exacerbates the undesired charge transfer issue).

Fig. 11 shows the efficiency and the final output voltage as a function of the frequency of the control signals.

Fig. 12 shows the efficiency and the final output voltage as a function of the supply voltage; all the charge pumps may be used in low voltage applications; if a more recent process (lower threshold voltages) is used, the minimum operating voltage of the charge pumps would be significantly lower.

IV. CONCLUSIONS

We have given conditions for determining if undesired charge transfer occurs in a given charge pump. These conditions may be used for designing new circuits less susceptible to this problem; as an example, a new charge pump has been proposed. In comparison with existing solutions, the additional circuit complexity is minimal; although a more complex timing strategy is necessary, the new charge pump offers both an higher final output voltage and a better efficiency if the transistor widths are enough large (see figure 10). At light load, the efficiency of the proposed circuit is much higher than the efficiency of classic circuit, thus significantly extending the battery lifetime (see the efficiency for large load resistors in fig. 9).

REFERENCES

- [1] R. St. Pierre, "Low power BiCMOS op amp with integrated current mode charge pump", JSSC, vol. 35, no. 7, July 2000, pp.1046-1050.
- [2] T. A. F. Duisters, E. C. Dijkmans, "A -90 dB THD rail-to-rail input op amp using a new local charge pump in CMOS", JSSC, vol. 33, no. 7, July 1998, pp.947-955.
- [3] R. Pelliconi, D. Iezzi, A. Baroni, M. Pasotti, P.L. Rolandi, "Power efficient charge pump in deep submicron standard CMOS technology", JSSC, vol. 38, no. 6, June 2003, pp.1068-1071.
- [4] D. Maksimovic, S. Dhar, "Switched-capacitor DC-DC converters for low-power on-chip applications", IEEE Power Electronics Specialists Conference, 1999, 27 June-1 July 1999, pp. 54 -59.
- [5] P. Favrat, P. Deval, M. J. Declercq, "A High Efficiency CMOS voltage doubler", JSSC, vol. 33, no. 3, March 1998, pp. 410-416.
- [6] C. Wang, J. Wu, "Efficiency improvement in charge pump circuits", JSSC, vol. 32, no. 6, June 1997, pp.852-860.

TABLE I

Reference parameters for the charge pumps CP1, CP2, CP3			
Parameter	CP 1 (fig. 1)	CP 2 (fig. 2)	CP 3 (fig. 6)
$w_n^{(a)}$	$300\mu\text{m}$	$150\mu\text{m}$	$300\mu\text{m}$
$w_p^{(b)}$	$690\mu\text{m}$	$345\mu\text{m}$	$690\mu\text{m}$
$w_{n,33}, w_{n,44}$	—	—	$2\mu\text{m}$
L (for all transistors)	$1.6\mu\text{m}$	$1.6\mu\text{m}$	$1.6\mu\text{m}$
C (pumping capacitors)	80pF	40pF	75pF
C_{33}, C_{44}	—	—	5pF
C_{LOAD}	80pF	80pF	80pF
R_{LOAD}	$40\text{k}\Omega$	$40\text{k}\Omega$	$40\text{k}\Omega$
f	5.3MHz	5.3MHz	5.3MHz
V_{DD}	2.5V	2.5V	2.5V
$w_{p,BNW}$ (n-well bias)	$10\mu\text{m}$	$5\mu\text{m}$	$10\mu\text{m}$
C_{BNW} (n-well bias)	5pF	5pF	5pF

a. width of all the N-MOSFETs but those which are separately specified
b. width of all the P-MOSFETs but those which are separately specified

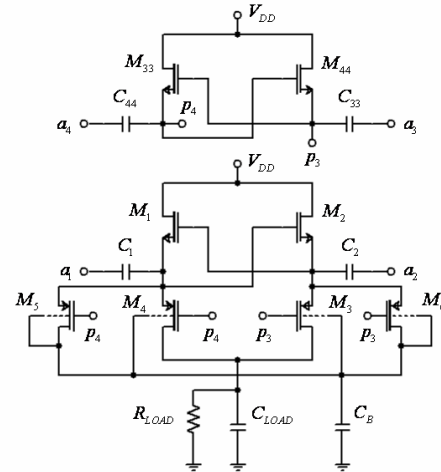


Figure 6. CP3: proposed charge pump.

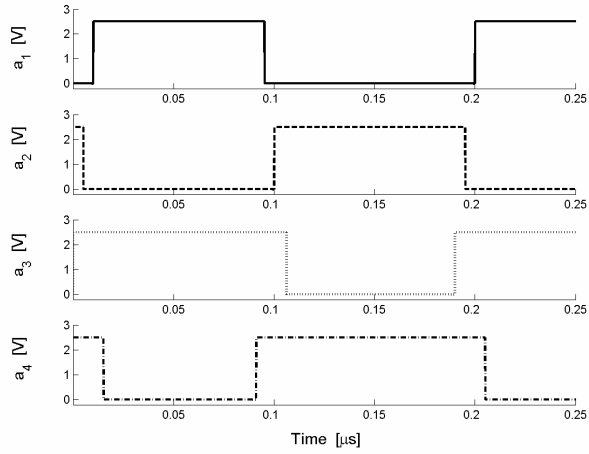


Figure 7. Control signals for the circuit in fig. 6.

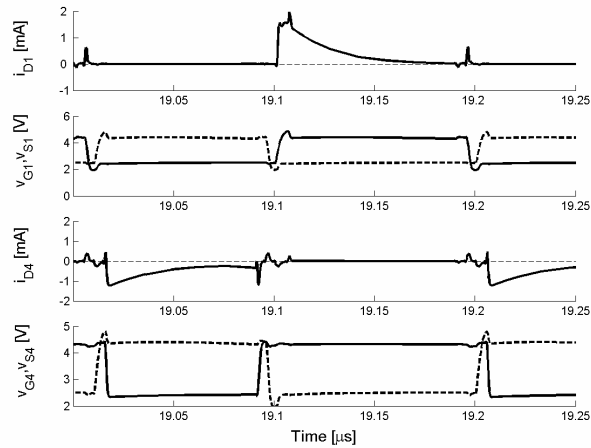


Figure 8. Simulated signals in the circuit in fig. 6.

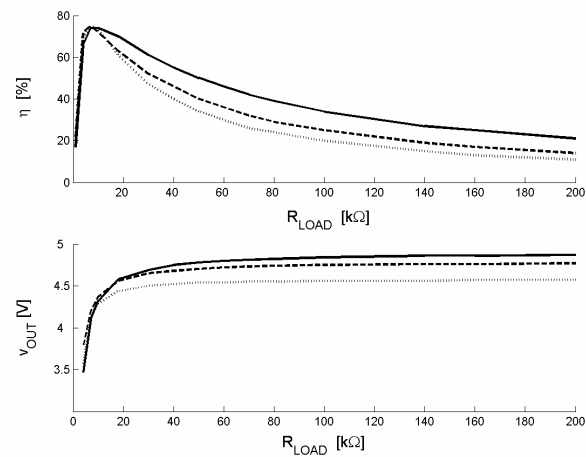


Figure 9. Efficiency and final output voltage of CP1 (dotted line), CP2 (dashed line), CP3 (solid line) vs. the load resistance R_{LOAD} .

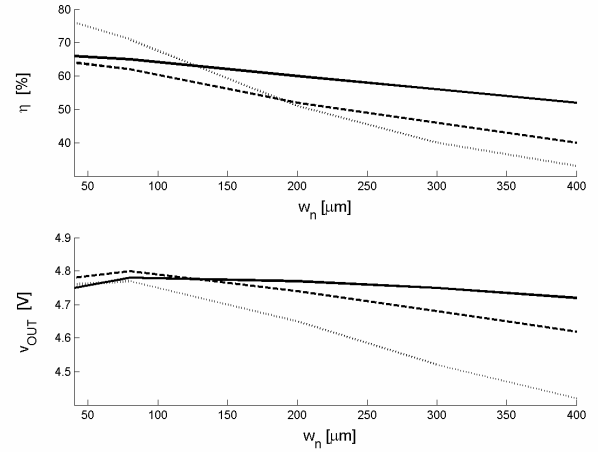


Figure 10. Efficiency and final output voltage of CP1 (dotted line), CP2 (dashed line), CP3 (solid line) vs. the transistor widths.

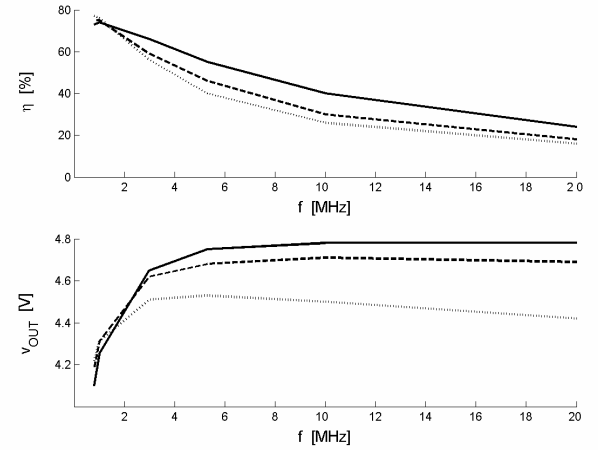


Figure 11. Efficiency and final output voltage of CP1 (dotted line), CP2 (dashed line), CP3 (solid line) vs. the operating frequency f .

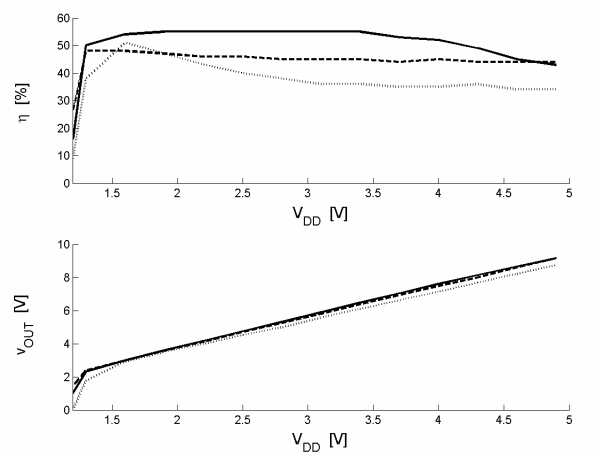


Figure 12. Efficiency and final output voltage of CP1 (dotted line), CP2 (dashed line), CP3 (solid line) vs. the supply voltage V_{DD} .